



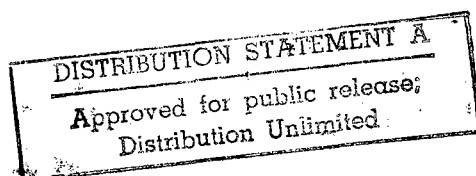
LASER INDUCED REACTION FOR PREBOND SURFACE PREPARATION OF ALUMINIUM ALLOYS

Stage 3 report (7-10/93)
Contract No. F61708-93-C005

by

M. Rotel, J. Zahavi
Israel Institute of Metals, Technion, Haifa, Israel

A. Buchman, H. Dodiuk
Materials and Processes Department,
RAFAEL, Haifa, Israel



1 9990216061

DIIC QUALITY INSPECTED 2

Haifa, January, 1994

AQF99-05-0923

REPORT DOCUMENTATION PAGE

Form Approved OMB No. 074-0188

Public reporting burden for this collection of information is estimated to average 1 hour per response, including the time for reviewing instructions, searching existing data sources, gathering and maintaining the data needed, and completing and reviewing this collection of information. Send comments regarding this burden estimate or any other aspect of this collection of information, including suggestions for reducing this burden to Washington Headquarters Services, Directorate for Information Operations and Reports, 1215 Jefferson Davis Highway, Suite 1204, Arlington, VA 22202-4302, and to the Office of Management and Budget, Paperwork Reduction Project (0704-0188), Washington, DC 20503

1. AGENCY USE ONLY (Leave blank)	2. REPORT DATE January 1994	3. REPORT TYPE AND DATES COVERED July-Oct 1993	
4. TITLE AND SUBTITLE Laser Induced Reaction for Prebond Surface Preparation of Aluminum Alloys. Stage 3.		5. FUNDING NUMBERS F61708-93-C005	
6. AUTHOR(S) Rotel, M.; Zahavi, J.; Buchman, A.; Dodiuk, H.			
7. PERFORMING ORGANIZATION NAME(S) AND ADDRESS(ES) Israel Institute of Metals Technion Research and Development Foundation Ltd. Haifa, Israel		8. PERFORMING ORGANIZATION REPORT NUMBER Materials and Processes Dept. Rafael Haifa, Israel	
9. SPONSORING / MONITORING AGENCY NAME(S) AND ADDRESS(ES) EOARD PSC802 Box 14 FPO 09499-0200		10. SPONSORING / MONITORING AGENCY REPORT NUMBER SPC 93-4019-3	
11. SUPPLEMENTARY NOTES			
12a. DISTRIBUTION / AVAILABILITY STATEMENT Approved for public release; distribution is unlimited.			12b. DISTRIBUTION CODE
13. ABSTRACT (Maximum 200 Words)			
14. SUBJECT TERMS Foreign Reports, EOARD			NUMBER OF PAGES 38
			16. PRICE CODE
17. SECURITY CLASSIFICATION OF REPORT UNCLASSIFIED	18. SECURITY CLASSIFICATION OF THIS PAGE UNCLASSIFIED	19. SECURITY CLASSIFICATION OF ABSTRACT UNCLASSIFIED	20. LIMITATION OF ABSTRACT UL

1. INTRODUCTION

The potential of UV laser irradiation as prebonding treatment of Al-2024 alloy was proved in a previous investigation(1) using a modified epoxy adhesive (2). Surface treatment of Al by excimer laser results in oxidation and morphological changes of the surface promoting shear adhesion strength when applying optimal laser conditions. The adhesion strength achieved by the laser treatment is similar or higher than chemically treated Al.

The objective of this research is to establish the effect of excimer ArF UV laser on the Al alloy surface microstructure and activity and to find its correlation with the macro behavior of shear strength and failure locus. The system treated was adhesively bonded Al joints with structural adhesives.

These adhesives are normally used in bonding and repairing processes for aerospace application. Surface treatment for bonding Al adherends with structural adhesives involve the use of harsh chemicals such as acids bases and organic solvents. Laser surface irradiation can therefore be used as an alternative, ecologically favorable treatment. In order to achieve high adhesive strength optimal laser parameters for the treatment should be chosen (repetition rate, energy and irradiation time).

The third stage of this research (0003 of the contract) is summarized in the present report. This stage includes the characterization of failure modes of the shear tested joints and the chemical changes of the Al substrate surface after irradiation. The results of the shear strength were reported in the previous stage and will be presented again in order to clarify the morphological results.

2. EXPERIMENTAL

2.1 Laser Treatment

The laser used during the course of this investigation is a UV excimer ArF (193 nm) laser EMG 201 MSC manufacture by "Lambda Physik", Germany. Beam cross section is 20mmx5mm with energy of 200mj/p*cm². Higher laser energies were achieved by reducing the laser beam area using focusing lens. Repetition rate was 30Hz and the number of pulses ranged between 1-5000. Specimen scanning is done by moving the specimen by means of a controlled x-y-z table. All experiments are conducted at ambient temperature and room environment. Fig 2.1 in the second stage report shows a schematic drawing and photo of the irradiation system.

2.2 Adherend and Adhesives

The adherend used throughout this work was an Al 2024-T3 alloy. The irradiated specimen were bonded by three different structural adhesives after primer application. Table 2.1 summarizes the data of the applied adhesives and the primers.

Table 2.1: The structural adhesives and primers

COMMERCIAL NAME (CYANAMID)	CURING CONDITIONS	APPLICATION FORM	SERVICE TEMPERATURE RANGE
FM73	1 Hr. 120 ⁰ C 40psi	FILM, 0.38mm POLYESTER CARRIER	-55 ⁰ C to +120 ⁰ C
FM3002K	1.5Hr. 120 ⁰ C 40psi	FILM, 0.3mm POLYESTER CARRIER	-55 ⁰ C to +175 ⁰ C
FM350NA	1Hr. 177 ⁰ C 30psi	FILM GLASS CARRIER	-65 ⁰ C to +177 ⁰ C
BR127 (chromate base)	1/2Hr. R.T. 1/2Hr. 121 ⁰ C	MIXING, BRUSHING	-55 ⁰ C to +177 ⁰ C
A187 (silane base)	1/2Hr. R.T. 1/2Hr. 90 ⁰ C	BRUSHING 2cc A187 in 80cc ethanol and 20cc D.I. water	- NA -

2.3 Testing

Adhesive joints properties were studied using Single Lap Shear joints (SLS) according to ASTM D-1002-72. The mode of failure was determined to be either adhesive (locus of failure in the adhesive/substrate interface) or cohesive (locus of failure within the adhesive matrix), or mixed. The surface of the irradiated area and the fracture surface morphology were studied by Scanning Electron Microscope (SEM) (Jeol model JMS 840, Japan) equipped with Energy Dispersive System (EDS, Link model 290).

2.4 Methodology

Two kinds of references are used in all the experiments: a non-treated Al 2024-T3 and an unsealed chromic acid anodized Al (according to MIL-A-8625C). The second reference is a conventional pre bonding treatment for aluminum alloy. The shear strength of the reference joints were tested with the same adhesives and primers as the laser treated joints. Primer application was carried out immediately after laser irradiation.

For optimization three treatment conditions were examined: laser treatment and primer BR127, laser treatment and primer A187 and laser treatment without primer. The adherends were kept in a desiccator between primer application and bonding, except during investigating the effect of open time.

3. RESULTS AND DISCUSSION

3.1 Failure Mode and Surface Morphology After Shear Testing.

Investigation of the effect of prebonding surface treatment with excimer laser was tested with three structural adhesives using Single-Lap-Shear joints (SLS).

Tables 3.1-3.5 summarize the optimization experiments with the three adhesives(1).

Table 3.1 summarizes the experimental results with primer BR127 and the three adhesives, table 3.2 summarizes the experimental results with primer A187 and adhesive FM73, table 3.3 summarizes experiments results with fresh primer BR127 and the adhesive FM73, table 3.4 summarizes experiments' results without primer and adhesive FM73 and table 3.5 summarizes experiments results with primer A187 and the three adhesives.

Table 3.1 shows that the highest lap shear strength for laser treated joints was achieved with FM73 adhesive .The shear strength of laser treated joints was 287Kg/cm² compared to 429Kg/cm² of the unsealed anodized joints and 128Kg/cm² of the untreated joints .Locus of failure for the laser treated joints with FM73 adhesive was cohesive as for anodized joints.

The shear strength of laser treated joints with the adhesives FM3002K and FM350NA and primer BR127 are low(100 and 92Kg/cm²), about 1/3 of the unsealed anodized joints (table 3.1). Locus of failure for the laser treated joints with FM300 2K and FM350 NA was adhesive while for unsealed anodized joints it was cohesive.

It should be noted that BR127 is not the primer advised for FM350 NA. The advised primer BR154 is on its way to our lab. and will be further investigated. The effect of heat cure on the laser treatment will also be investigated as a probable reason for the reduced strength of the high temperature structural adhesives.

Figs. 3.1-3.7 show the morphology of the failure surface of the shear joints the strength of which were summerized in table 3.1.

Figs. 3.1-3.3 show the failure surface after SLS tests for joints with the adhesive FM73 and primer BR127. Comparison between the cohesive failure of the anodized adherends and the adhesive failure of the untreated adherends is shown in fig.3.1.

The cohesive failure is localized within the adhesive. The carrier net and the matrix adhesive are present on both surfaces.

The adhesive failure is localized in the interface between the adhesive and the aluminum adherent. The metal surface is exposed on one adherend and a smooth surface of the adhesive is observed on the opposite one.

Figs 3.2-3.3 are SEM photographs of the laser treated joint failure surfaces after SLS tests. It can be seen that increasing the number of laser pulses resulted in increasing cohesive failure area. Irradiation with 600 and 1000 pulses resulted in mixed adhesive/cohesive failure (fig. 3.2) while irradiation with 2000 pulses resulted in a fully cohesive failure (fig.3.3).

Figs. 3.4-3.5 show the failure surface after SLS tests with the adhesive FM300K and primer BR127. Comparison between the cohesive failure of the anodized adherends and the adhesive failure of the untreated adherends is shown in fig.3.4.

The failure mode of the laser treated adherends (fig.3.5) is adhesive even at high number of pulses. This mode of failure is one of the reasons for the low shear strength obtained (table 3.1).

Figs. 3.6-3.7 show the failure surface after SLS tests with the adhesive FM350NA and primer BR127. Comparison between the cohesive failure of the anodized adherends and the adhesive failure of the untreated adherends is shown in fig.3.6.

The failure mode of the laser treated adherends (fig.3.7) is adhesive even at high number of pulses.

Applying a different kind of primer, silane based A187 with the three structural adhesives improved the failure mode and shear strengths. Tables 3.2-3.3(1) summarize these results and figs.3.8 - 3.11 present the failure morphology. The mode of failure for the laser treated adherends was cohesive (within the adhesive) for FM73 and FM300 2K and adhesive for FM350NA.

Best results were reached with the adhesive FM73 possibly due to its better compatibility with the primer A187 and its low curing temperature.

The highest shear strength for laser treated joints was 344Kg/cm² (tables 3.2-3.3) compared to 398Kg/cm² with unsealed chromic anodized joints.

Shear strengths of laser treated joints with adhesives FM350NA and FM300 2K and primer A187 reached values of

217Kg/cm² and 294Kg/cm², respectively (table 3.3), compared to 249 Kg/cm² and 305Kg/cm², respectively, for unsealed chromic anodized joints. The values of shear strength are close to those of laser treated joints (table 3.3).

The locus of failure for laser treated joints is cohesive with FM300 2K and is adhesive with FM350NA). For the adhesive FM350NA another primer will be applied (BR154), further on.

Figs. 3.8 -3.11 show the failure surface morphology of SLS adherends of joints bonded with FM350NA and primer A187. Comparison between the cohesive failure of the anodized adherends and the adhesive failure of the untreated adherends is shown in fig.3.8.

The failure mode of the laser treated adherends (fig.3.9 -3.11) with FM350NA and primer A187 is adhesive even at high number of pulses, probably due to incompatibility of the primer and the high curing temperature of the adhesive.

Experiments with a fresh BR127 primer and the adhesive FM73 (table 3.4) show that laser treated joints have shear strength similar to those with the primer A187 (329 Kg/cm²). Figs 3.12-3.13 show the cohesive failure mode of laser treated joints bonded with fresh BR127 and FM73. Experiments without a primer (table 3.5) and with an adhesive FM73 show shear strength of 321 Kg/cm². These results prove that the main effect of the surface treatment and improve adhesion strength arise from the laser irradiation while the primer has only a minor effect.

The effect of oxygen atmosphere during laser irradiation was also tested. It seems that oxygen has little effect of lowering adhesion strength (not as expected). A similar effect was observed in an earlier research (6). The reason is probably due to the reaction of oxygen with the active sites formed during laser irradiation, thus decreasing surface activity.

Table 3.1: Adhesive shear strength for three structural adhesives with primer BR127. Laser energy 180mj/p*cm²

SAMPLE	PULSE NO.	ADHESIVE	S.L.S Kg/cm ²	FAILURE MODE
UNTREATED		FM300K	39.5±3	a
ANODIZED			305.6±25	m
LASER TREATED	600		88.0±8	a
	1000		86.8±20	a
	2000		101.3±15	a
UNTREATED		FM73	127.7±19.4	c
ANODIZED			428.6±5.7	c
LASER TREATED	600		286.8±16.4	m
	1000		280.5±15.5	m
	2000		286.9±4.6	c
UNTREATED		FM350NA	55.2±5.3	a
ANODIZED			264.1±15.3	c
LASER TREATED	600		92±8.7	a
	1000		86.1±12.5	a
	2000		77.5±5.5	a

c - cohesive failure
a - adhesive failure
m - mixed failure

Table 3.2: Adhesive shear strength - adhesive FM73, primer A187- with and without oxygen during laser irradiation. Laser energy 180mj/p*cm².

SAMPLE	PULSE NO.	ADHESIVE	S.L.S Kg/cm ²	FAILURE MODE	
UNTREATED		FM73	303.4±6.4	c	
ANODIZED			393.9±18	c	
LASER TREATED	100		301.4±1.7	c	WITHOUT OXYGEN
	600		316±15.8	c	
	1000		334±10.7	c	
	2000		319±9.6	c	
LASER TREATED	100		310.7	c	WITH OXYGEN
	600		298.4±2.2	c	
	2000		298±7.6	c	

c - cohesive failure
a - adhesive failure
m - mixed failure

Table 3.3: Adhesive shear strength for three structural adhesives primer A187. Laser energy 180mj/p*cm²

ADHESIVE	FM73	FM3002K	FM350NA
SAMPLE	S.L.S Kg/cm ²	S.L.S Kg/cm ²	S.L.S Kg/cm ²
UNTREATED	303.4±6.4(C)		103±3(A)
ANODIZED	393.9±18(C)		249±17(A)
LASER TREATED			
1000 PULSES	325.7±28(C)	294.5±7(C)	217±29(A)
2000 PULSES	344.3±12.8(C)	207±30(C)	190±5(A)
5000 PULSES	330.5±13(C)	289±32(C)	182±28(A)

c - cohesive failure
a - adhesive failure
m - mixed failure

Table 3.4: Adhesive shear strength -adhesive FM73, primer fresh BR127.

SAMPLE	PULSE NO.	ADHESIVE	S.L.S Kg/cm ²	FAILURE MODE
UNTREATED		FM73	127.7±9.4	c
ANODIZED			428.6±1.7	c
LASER TREATED	1000 180mj/p*cm ²		329.6±12	c
	100 1J/p*cm ²		312±29	

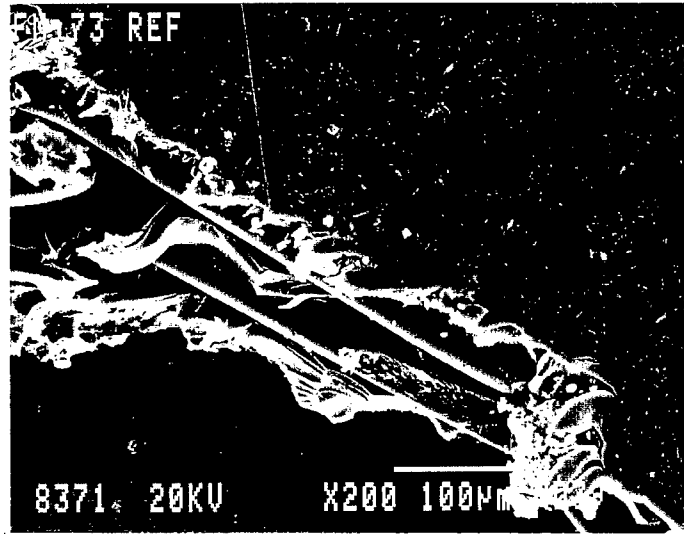
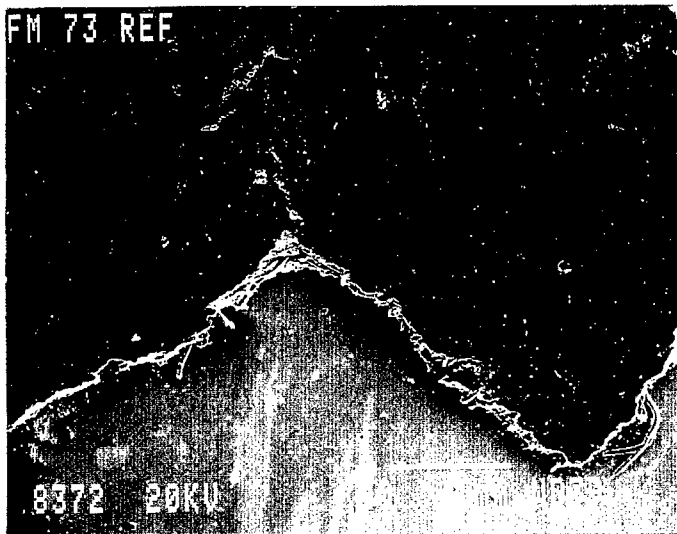
c - cohesive failure
a - adhesive failure
m - mixed failure

Table 3.5: Adhesive shear strength -adhesive FM73, without primer. Laser energy 180mj/p*cm².

SAMPLE	PULSE NO.	ADHESIVE	S.L.S Kg/cm ²	FAILURE MODE
ANODIZED	--	FM73	370±7.7	c
LASER TREATED	600	FM73	302±15	c
	1000		302±14	c
	2000		321±4.5	c

c - cohesive failure

a



b

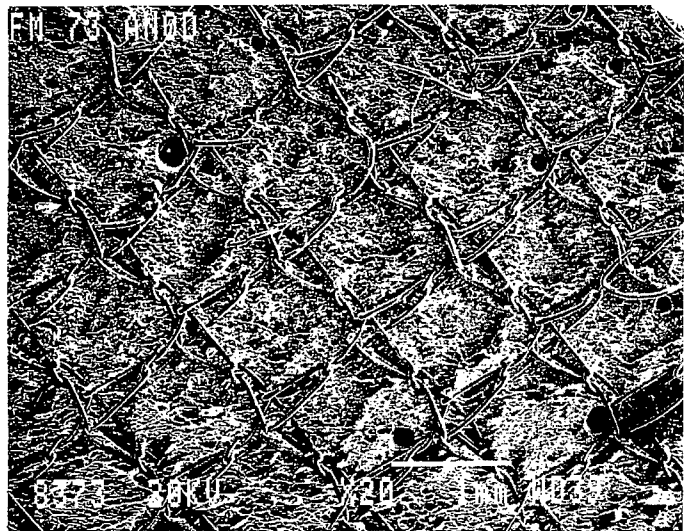
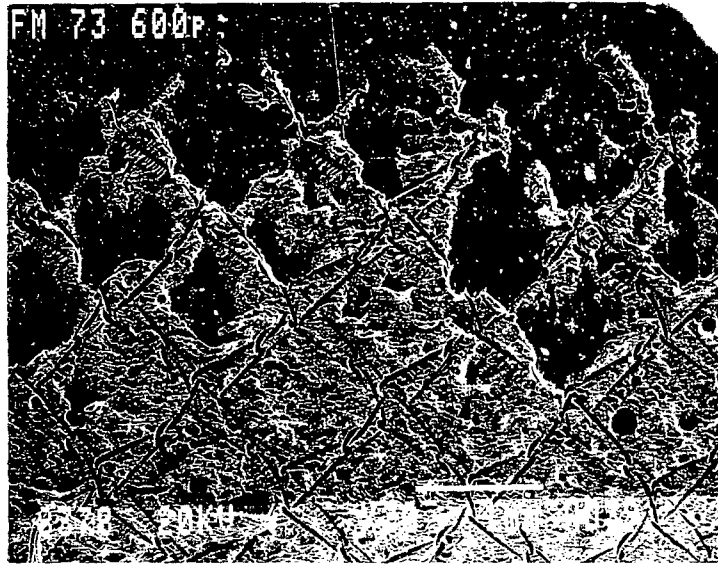


Fig. 3.1: SEM photographs of the surface failure morphology of SLS tests (table 3.1) with adhesive FM73, primer BR127. a: without treatment. b: anodized adherends.

a



b

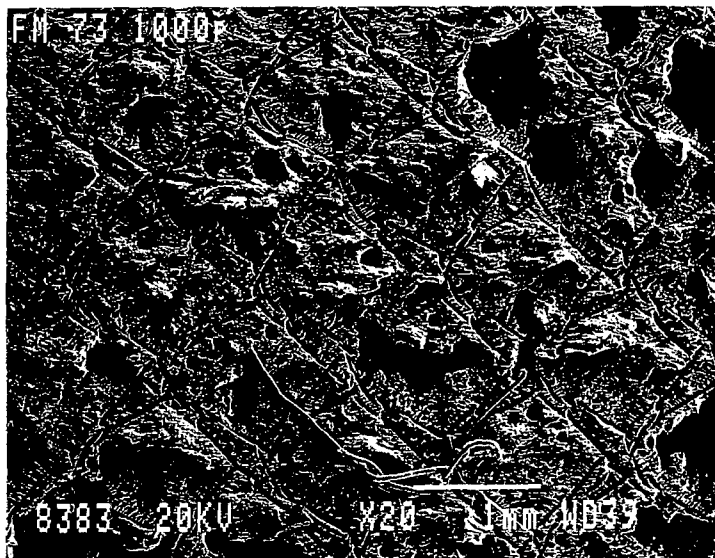


Fig. 3.2: SEM photographs of the surface failure morphology of SLS joints (table 3.1) with adhesive FM73, primer BR127, laser energy $180\text{mj/p}\cdot\text{cm}^2$ a: laser treated adherends, 600 pulses. b: laser treated adherends, 1000 pulses.

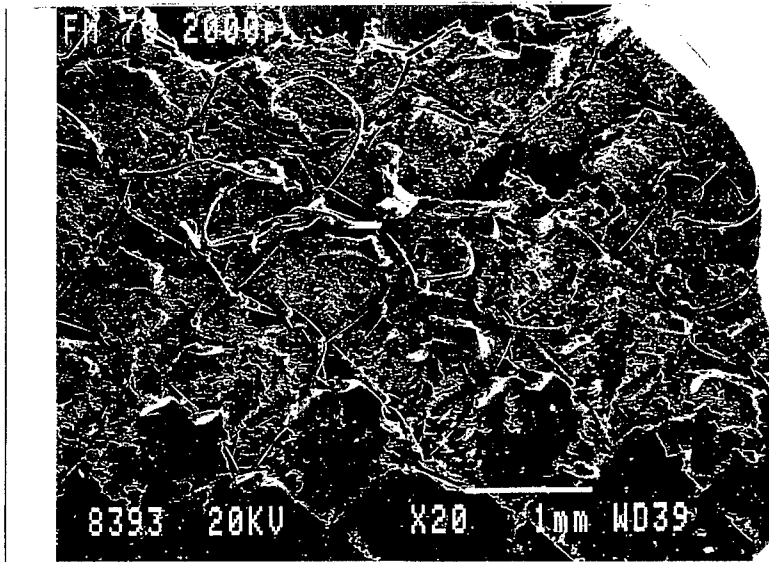
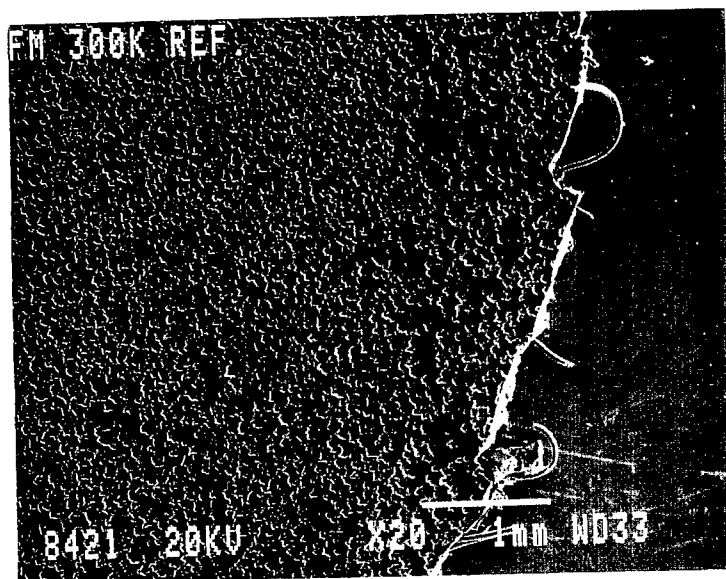


Fig. 3.3: SEM photographs of the surface failure morphology of SLS joints (table 3.1) adhesive FM73, primer BR127, laser treated adherends, 2000 pulses, 180mj/p*cm².

a



b

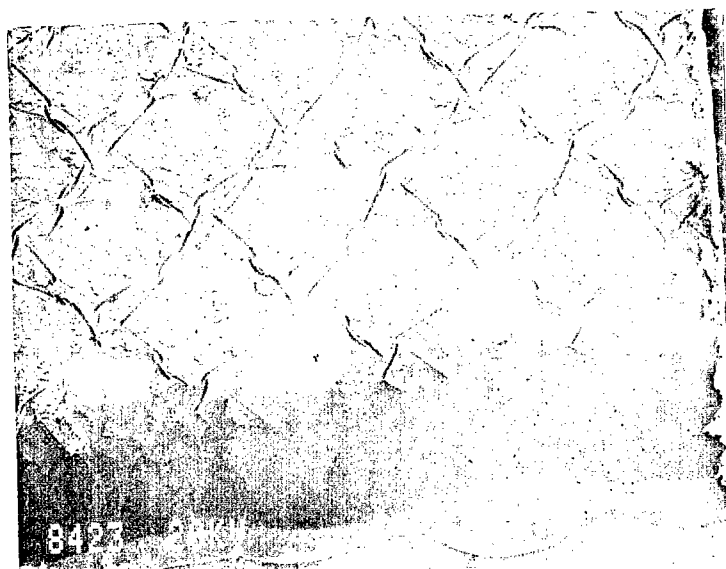
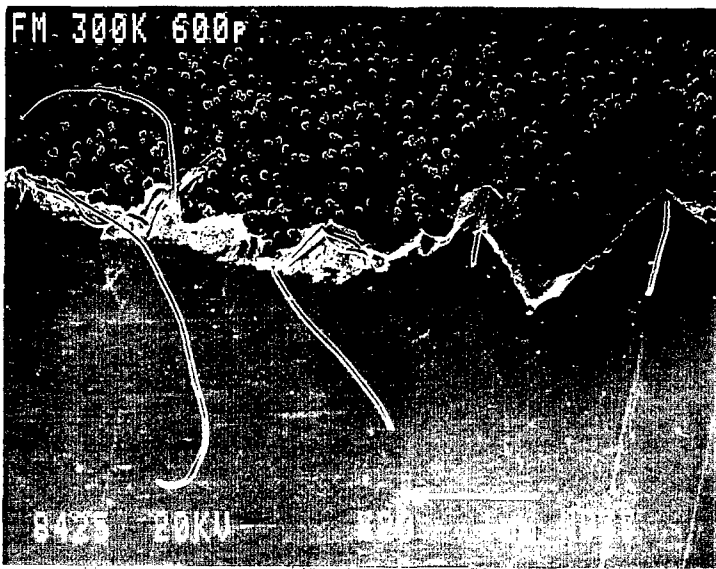
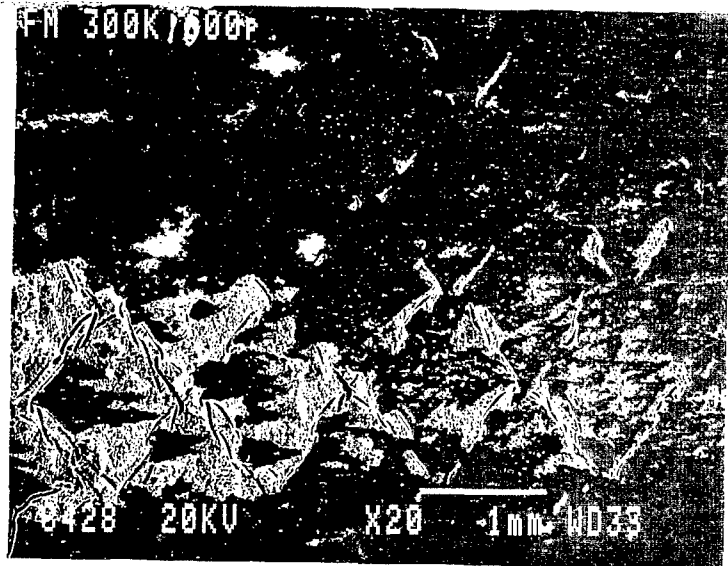


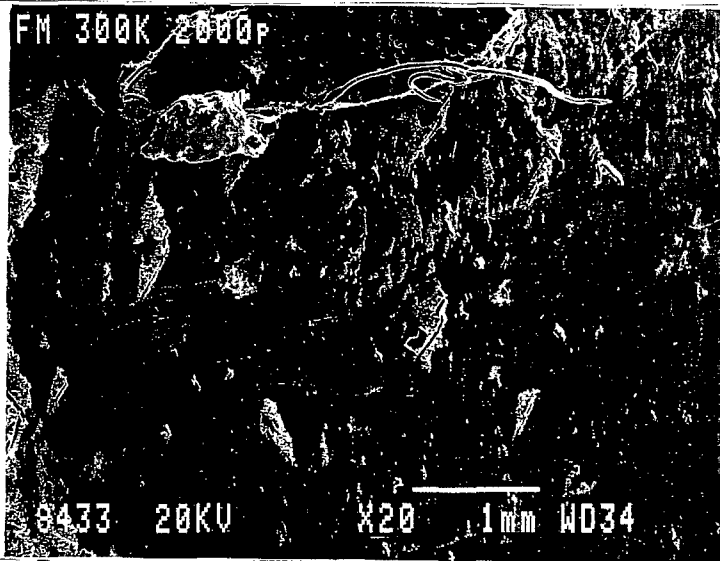
Fig. 3.4: SEM photographs of the surface failure morphology of SLS joints (table 3.1) with adhesive FM3002K, primer BR127.a: without treatment. b: anodized adherends.



a



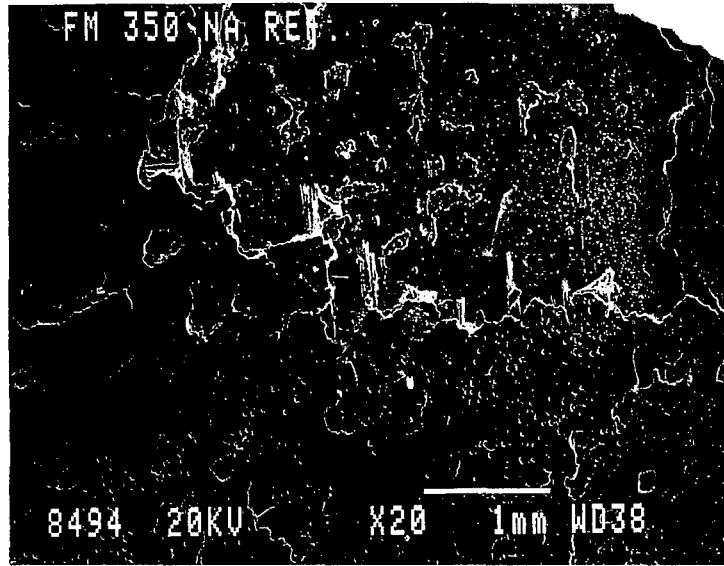
b



c

Fig. 3.5: SEM photographs of the surface failure morphology of SLS joints (table 3.1) with adhesive FM3002K, primer BR127, laser energy $180\text{mj/p}\cdot\text{cm}^2$ a: laser treated adherends, 600 pulses. b: laser treated adherends, 1000 pulses. c: laser treated adherends, 2000 pulses.

a



b

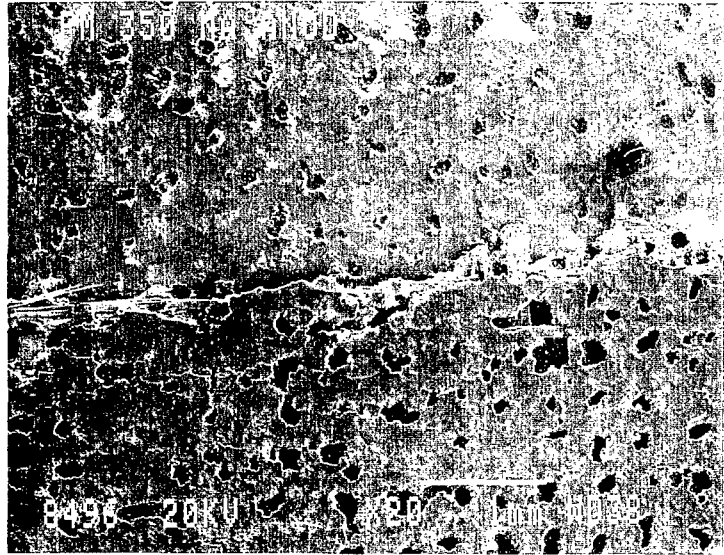
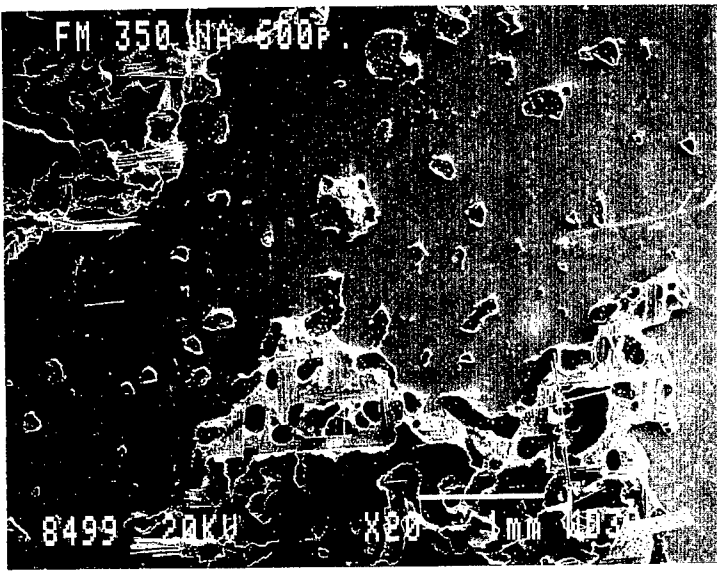
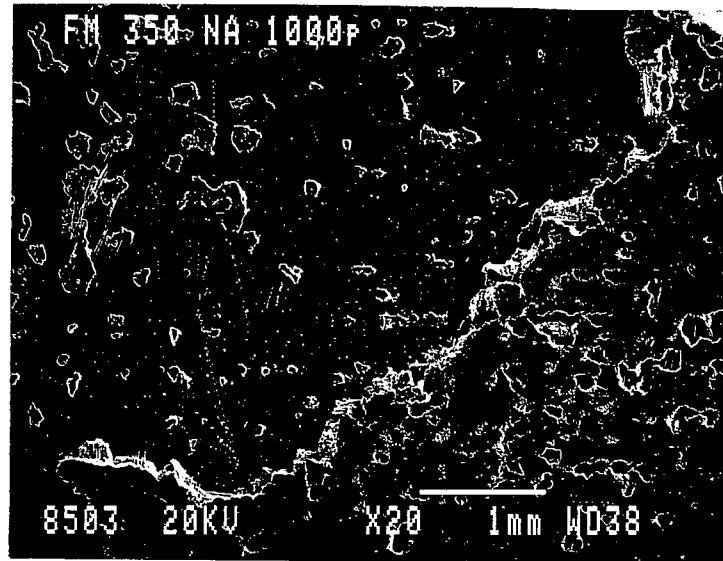


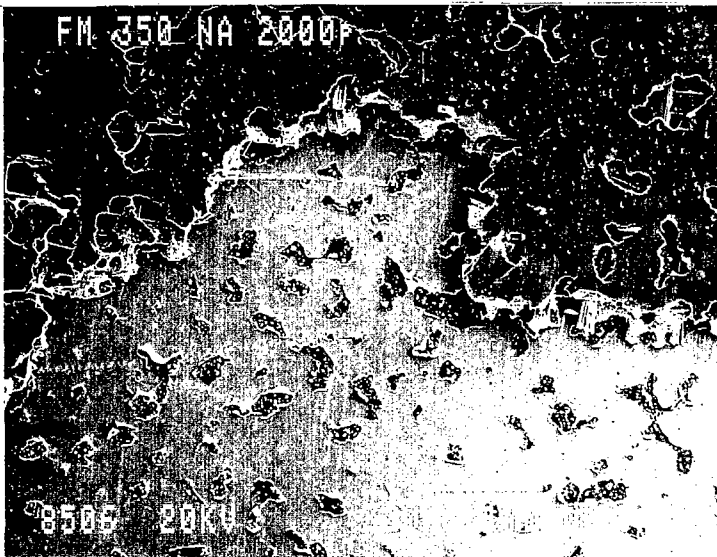
Fig. 3.6: SEM photographs of the surface failure morphology of SLS joints (table 3.1) with adhesive FM350NA, primer BR127. a: reference adherends without treatment. b: reference adherends - anodized adherends.



a



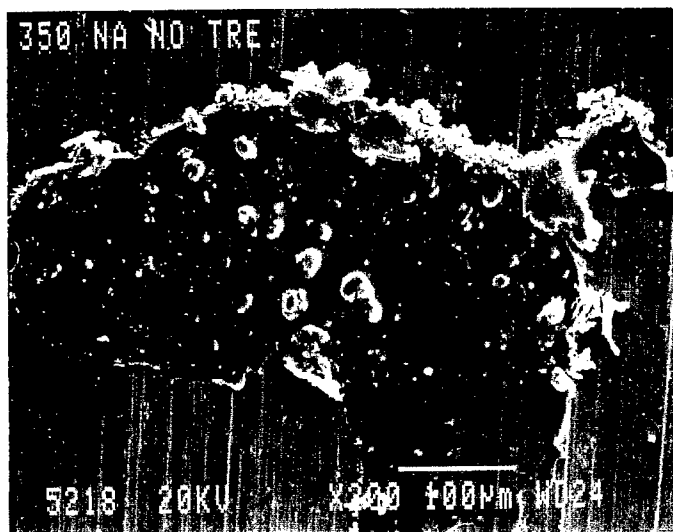
b



c

Fig. 3.7: SEM photographs of the surface failure morphology of SLS joints (table 3.1) with adhesive FM350NA, primer BR127, laser energy $180\text{mj/p}\cdot\text{cm}^2$ a: laser treated adherends, 600 pulses. b: laser treated adherends, 1000 pulses. c: laser treated adherends, 2000 pulses.

a



b

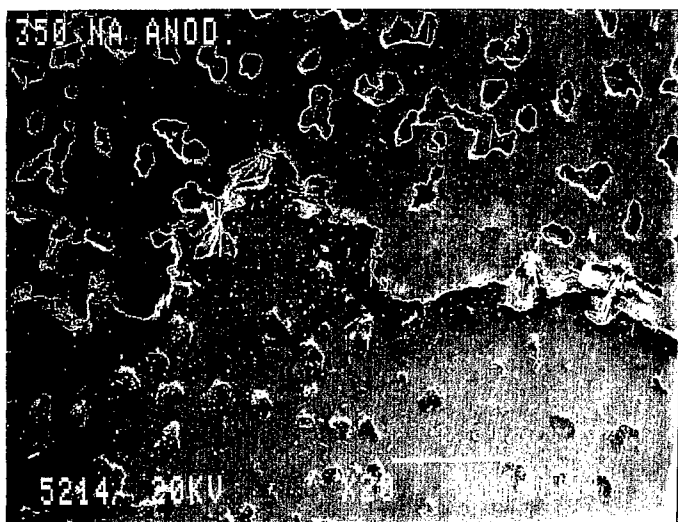


Fig. 3.8: SEM photographs of the surface failure morphology of SLS joints (table 3.3) with adhesive FM350NA, primer A187. a: without treatment. b: anodized adherends.

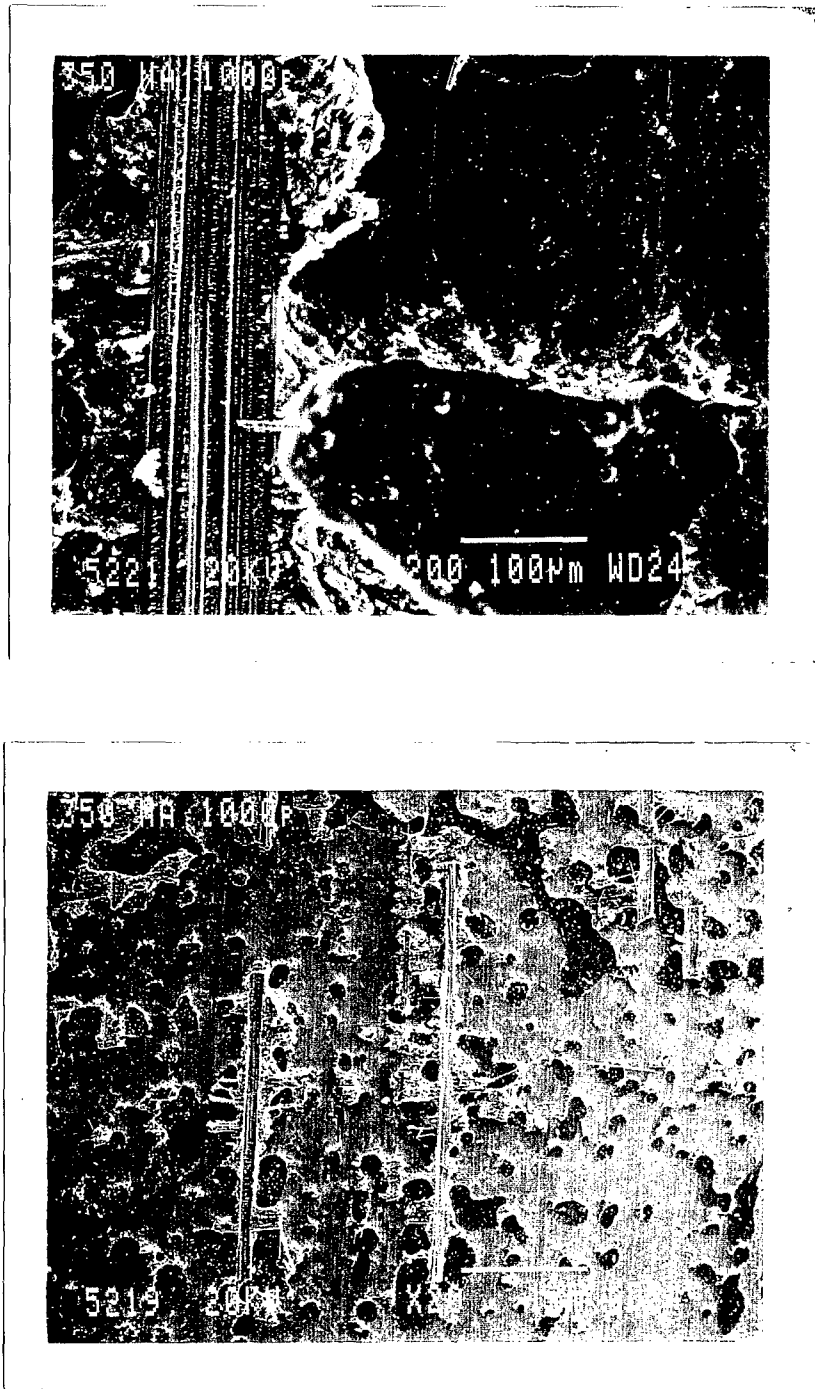


Fig. 3.9: SEM photographs of the surface failure morphology of SLS joints (table 3.3) with adhesive FM350NA, primer A187, laser energy $180\text{mj/p}^*\text{cm}^2$, 1000 pulses.

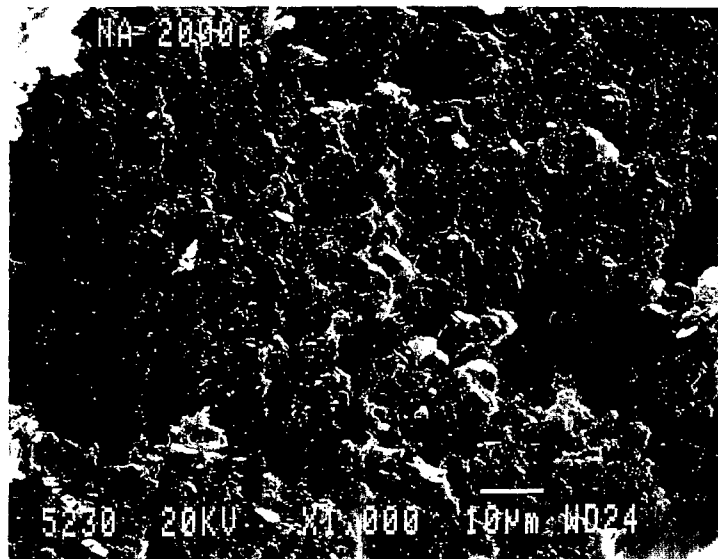
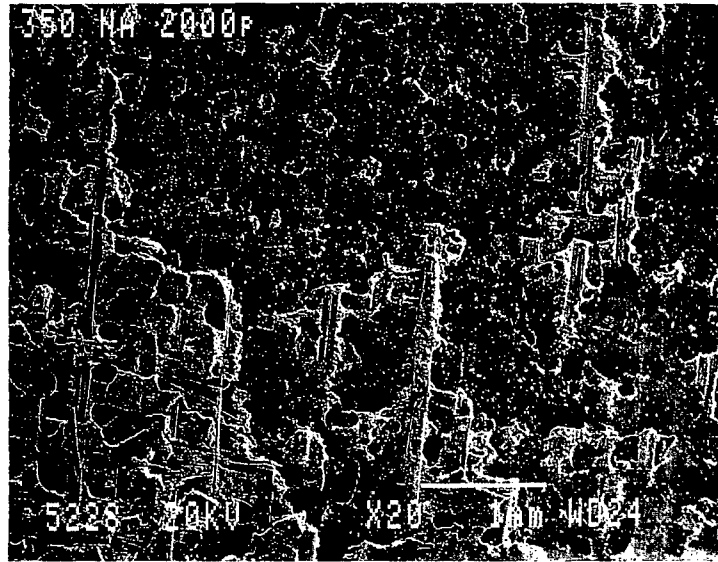


Fig. 3.10: SEM photographs of the surface failure morphology of SLS joints (table 3.3) with adhesive FM350NA, primer A187, laser energy $180\text{mj/p}\cdot\text{cm}^2$, 2000 pulses.

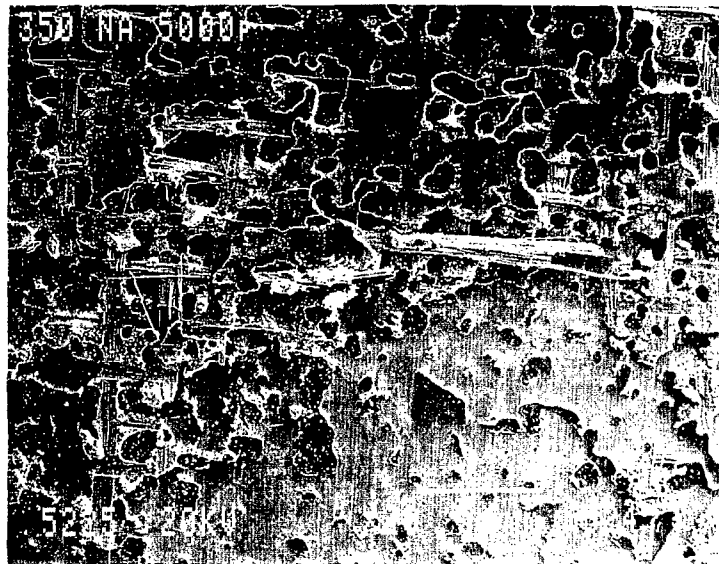


Fig. 3.11: SEM photographs of the surface failure morphology of SLS joints (table 3.5) with adhesive FM350NA, primer A187, laser energy $180\text{mj/p}\cdot\text{cm}^2$, 5000 pulses.

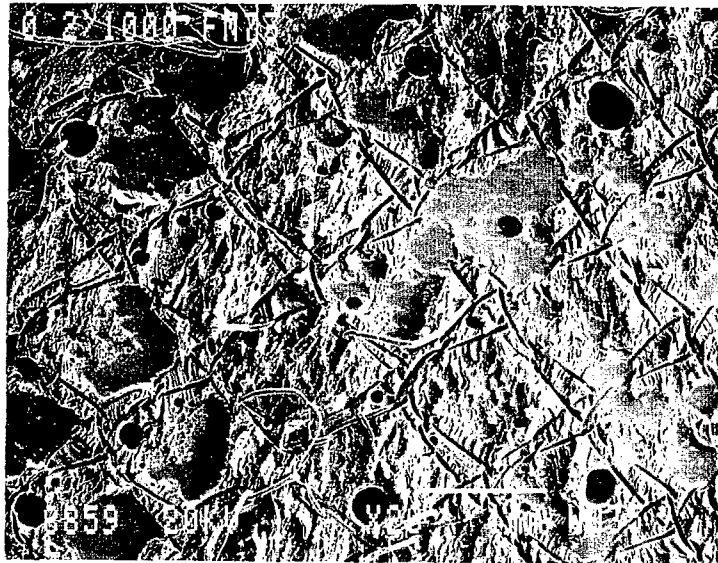


Fig. 3.12: SEM photographs of the surface failure morphology of SLS joints (table 3.4) with adhesive FM73, fresh primer BR127, laser energy $180\text{mj/p}\cdot\text{cm}^2$, 1000 pulses.

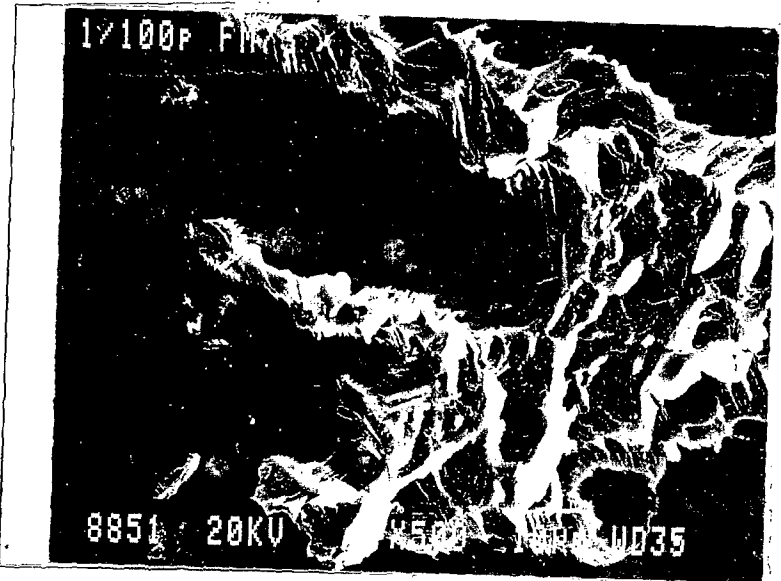
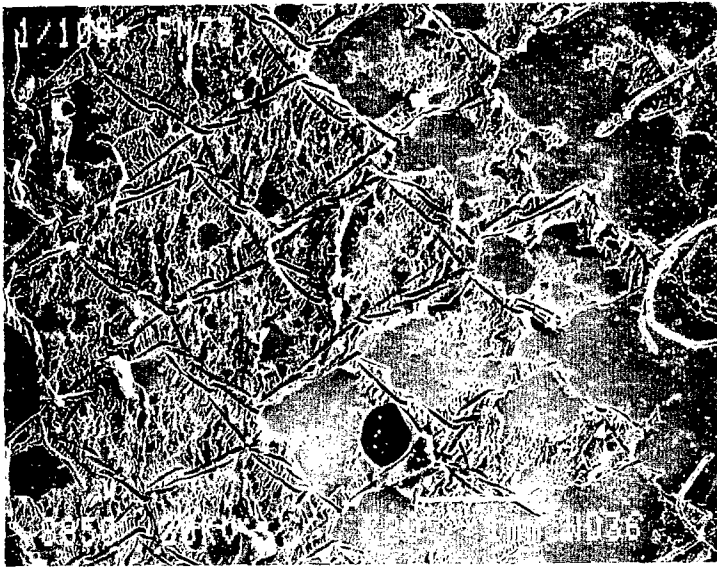


Fig. 3.13: SEM photographs of the surface failure morphology of SLS joints (table 3.4) with adhesive FM73, fresh primer BR127, laser energy $1\text{J}/\text{p}\cdot\text{cm}^2$, 100 pulses.

3.2 INFRA-RED SPECTROSCOPY

Figs. 3.14 -3.15 are FTIR spectra of laser treated aluminum adherend. The adherends were cleaned by degreasing process before laser irradiation. The irradiation was carried out in air with and without oxygen.

Fig.3.14 is the spectra of the irradiated adherends (400cm^{-1} - 4000cm^{-1}) and fig.3.15 is enlargement of the spectra in the range 400cm^{-1} - 2000cm^{-1} . The absorbance peaks shown in these figs. are:

1. around 3200cm^{-1} Al-O-H + H₂O (stretch) (2,3)
2. around 1600cm^{-1} Al-O-H₂O (stretch) absorbed water molecules (2,3)
3. 1450cm^{-1} Al-O (stretch) (2,3)
4. 1119cm^{-1} , 1100cm^{-1}
5. 1072cm^{-1}
6. 950cm^{-1}
7. 792cm^{-1}
8. 612cm^{-1}
9. 520cm^{-1}
10. 460cm^{-1}

The peaks at the wavelength range $400-1100\text{cm}^{-1}$ belong to various hydroxides (4,5) as indicated in figs. 3.16, 3.17.

The spectrum of the specimen irradiated under oxygen stream differ from the spectrum of the specimen that was irradiated without oxygen stream (figs. 3.14, .3.15).

Comparison between fig. 3.15a and fig. 3.15b show more defined peaks at 1600cm^{-1} , 1450cm^{-1} , 1416cm^{-1} and 1362cm^{-1} for the spectrum of the specimen irradiated without oxygen. This result proves the assumption that the oxygen probably reacts with the active sites reducing their concentration and the chemical activity of the surface .

A new peak at 660cm^{-1} appeared at oxygen atmosphere typical to oxygen rich hydroxide (AlOOH).

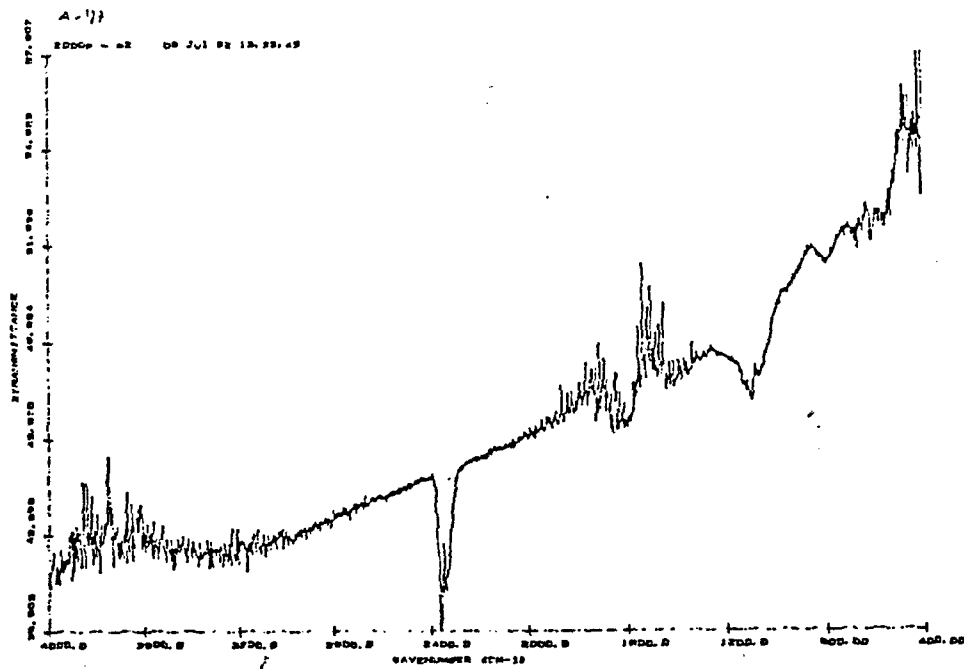
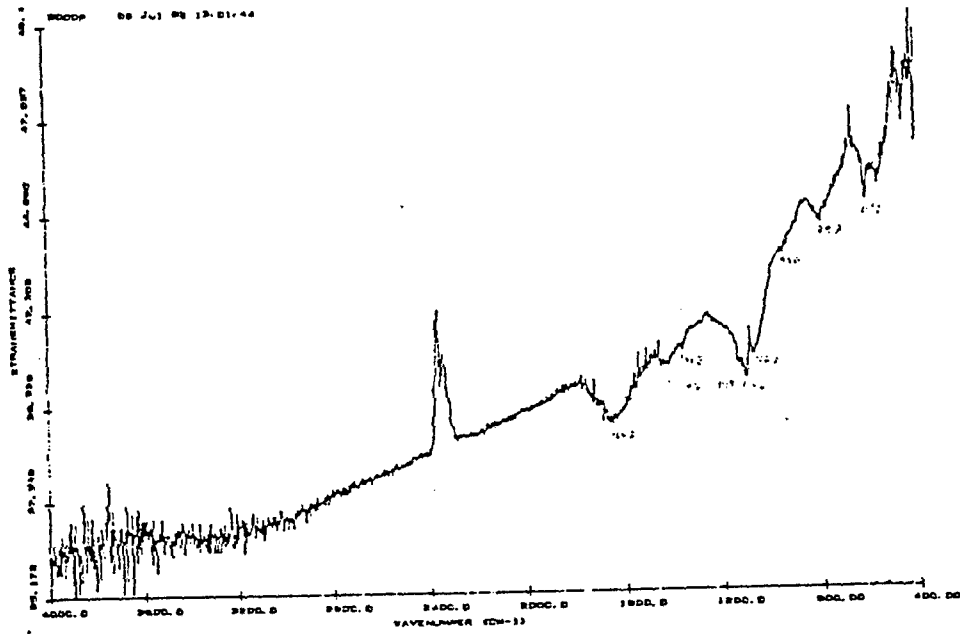


Fig.3.14: FTIR spectra of irradiated aluminum. Laser energy $0.18\text{ j/p}\cdot\text{cm}^2$, 2000 pulses. a. without oxygen stream. b. with oxygen steam.

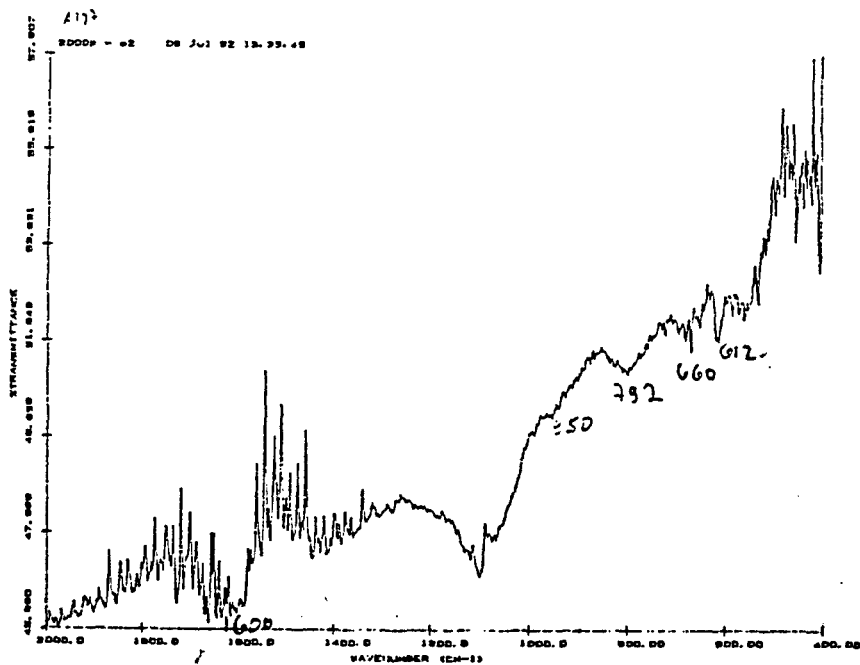
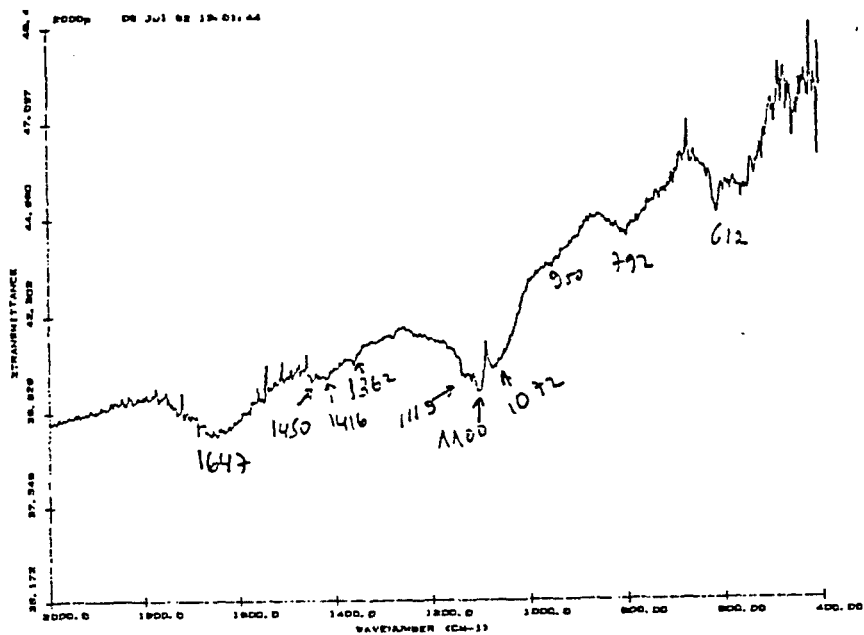


Fig. 3.15: Enlargement of FTIR spectra of fig.3.14 at the wavelength range of 2000-400cm⁻¹. a. without oxygen stream. b. with oxygen stream.

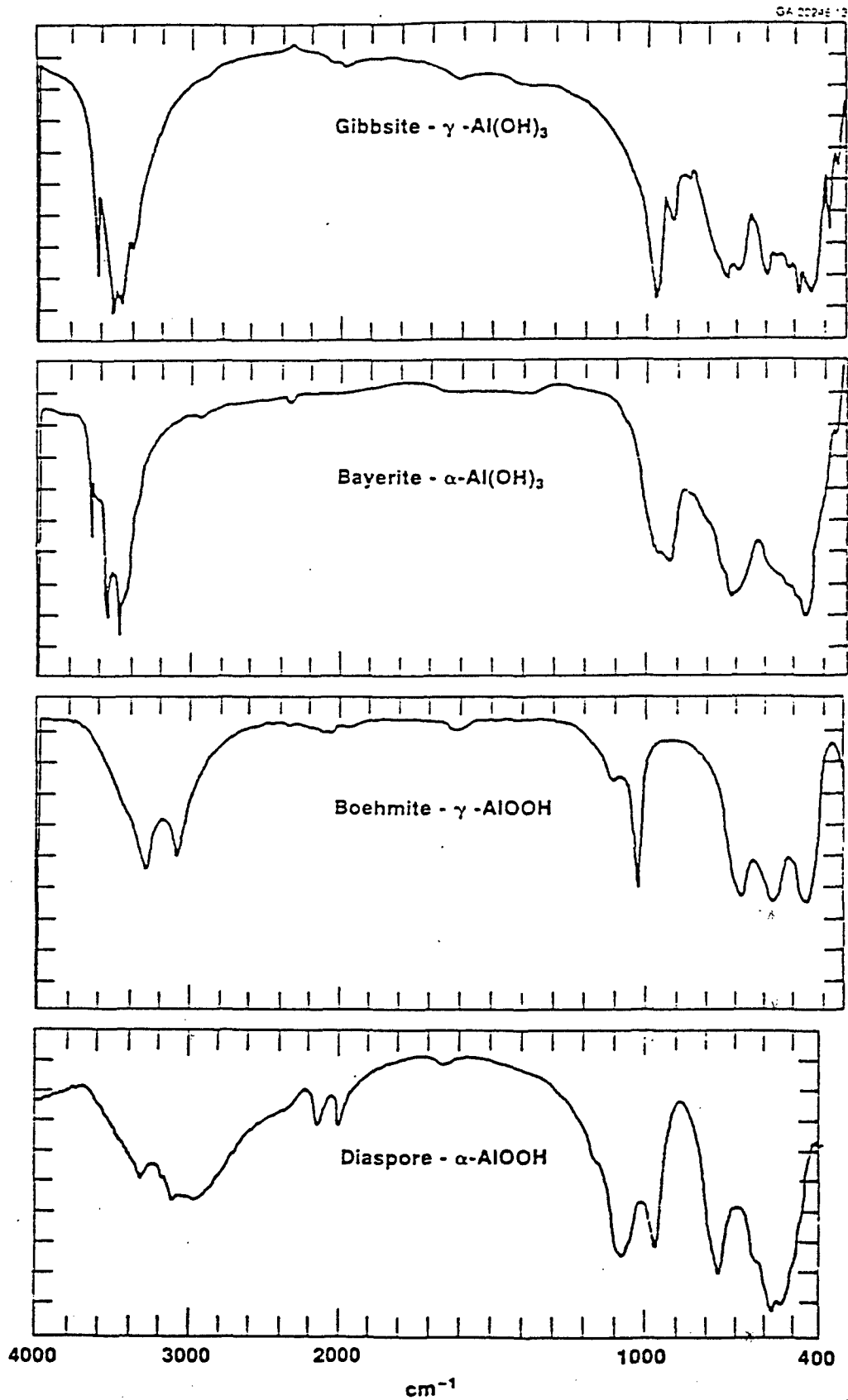


Fig.3.16: Infra Red spectra of various aluminum hydroxide(4).

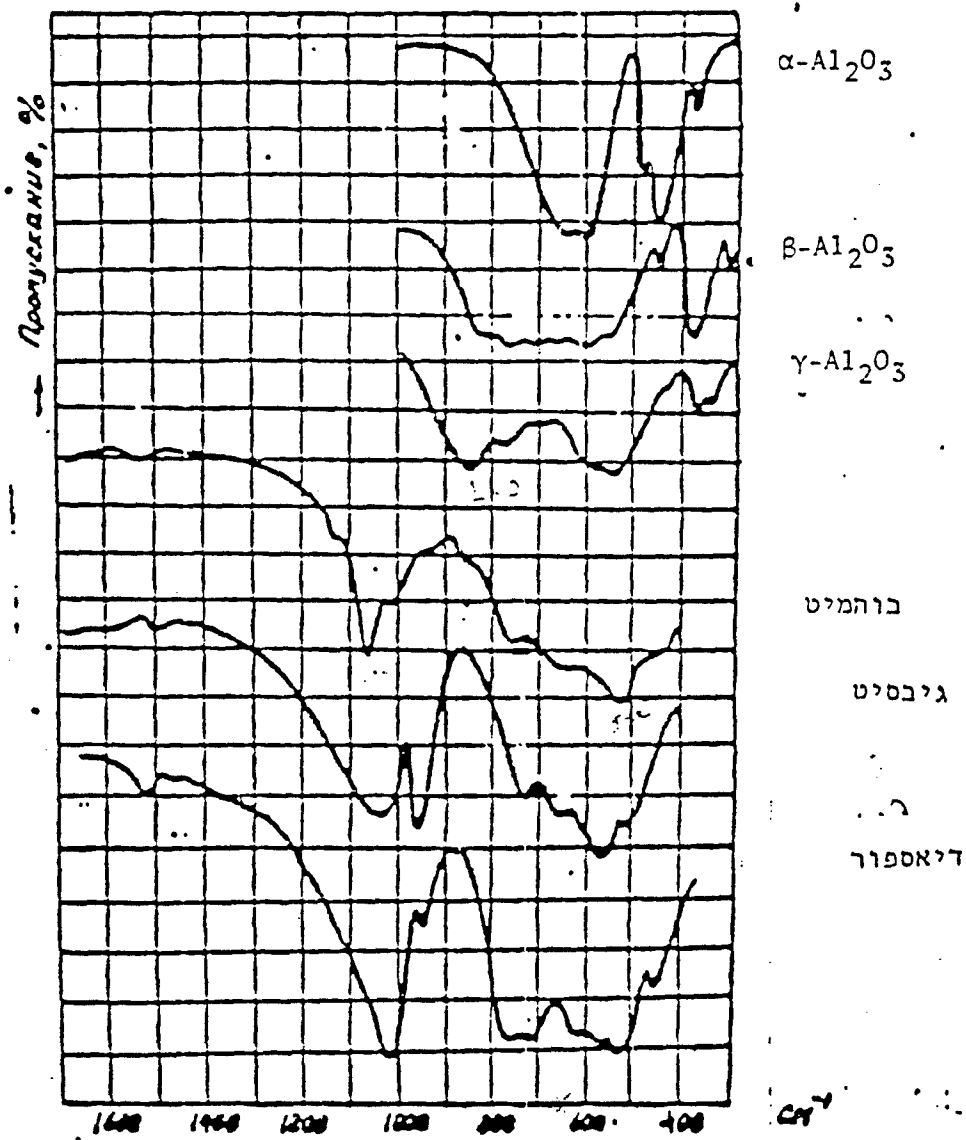


Fig.3.17: Infra Red spectra of aluminum oxides and hydroxides (5).

3.3 Auger Spectroscopy

Aluminum samples irradiated at various laser conditions were examined by auger spectroscopy in order to study the effect of laser energy and number of pulses on the surface chemical composition. SEM and FTIR analysis were also conducted to complete the information and gain better understanding. Figs. 3.18-3.22 present auger depth profiles of the aluminum specimen.

Fig. 3.18 shows the depth profile of the untreated aluminum. The major component formed on the Al surface was carbon which also penetrated the oxides of aluminum and magnesium. The carbon originated probably from organic contaminations.

Fig.3.19 shows the auger depth profiles of Al specimen treated at laser energy of $0.18\text{J/p}\cdot\text{cm}^2$ with 2000 and 5000 pulses. The major components on the surface were oxygen, aluminum and magnesium. Carbon was absent in the surface which proves the cleaning process of the laser. The magnesium and aluminum oxide layers of the specimen irradiated with 2000 pulses was thicker (about 580Å) than the oxides layer of the specimen irradiated with 5000 pulses (about 270Å) probably due to ejection of volatile at longer irradiation periods. Irradiation at this energy level ($0.18\text{J/p}\cdot\text{cm}^2$) did not produce morphological changes at the Al surface.

Fig. 3.20 shows the auger depth profiles of Al specimen treated at laser energy of $0.57\text{J/p}\cdot\text{cm}^2$ with 10 and 1000 pulses. The oxides layers at this energy level were thicker (about 900Å) than those produced at laser energy of $0.18\text{J/p}\cdot\text{cm}^2$.

Fig. 3.21 shows the auger depth profiles of Al specimen treated at laser energy of $1\text{J/p}\cdot\text{cm}^2$ with 10 and 1000 pulses. Irradiation with 10 pulses resulted in oxide layers of Al and Mg with thickness of about 700Å probably due to ablation. Irradiation with 1000 pulses resulted in aluminum oxide layer (without Mg) in which the relationship between Al and oxygen was as in Al_2O_3 , i.e. O: 60% and Al: 30%.

Fig.3.22 shows the auger depth profiles of specimen treated at laser energy of $2.7\text{J/p}\cdot\text{cm}^2$ with 10, 50 and 100 pulses. Irradiation at this energy level resulted in introduction of nitrogen into the upper surface layer (Al nitration). The nitrogen content increased to 25-30% at the depth of 60Å and 20Å (for 10 pulses irradiation and 50 or 100 pulses irradiation, respectively) and then decrease to 10% and less at the depth of 150Å . The oxygen

content decreased from 30% at the surface to less than 10% at the depth of 150 Å.

The above auger results show that different processes occurred at various laser energies and time. A more detailed explanation of the phenomena will be given when further experiments will be conducted.

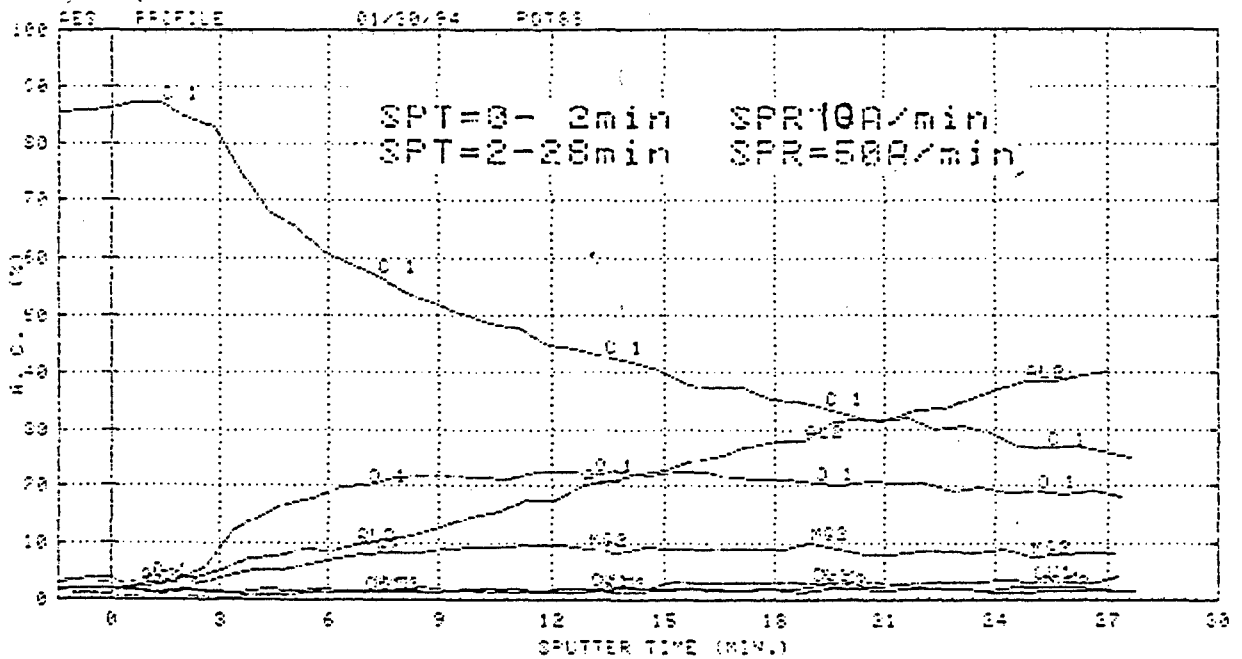


Fig.3.18: Auger depth profile of untreated aluminum.

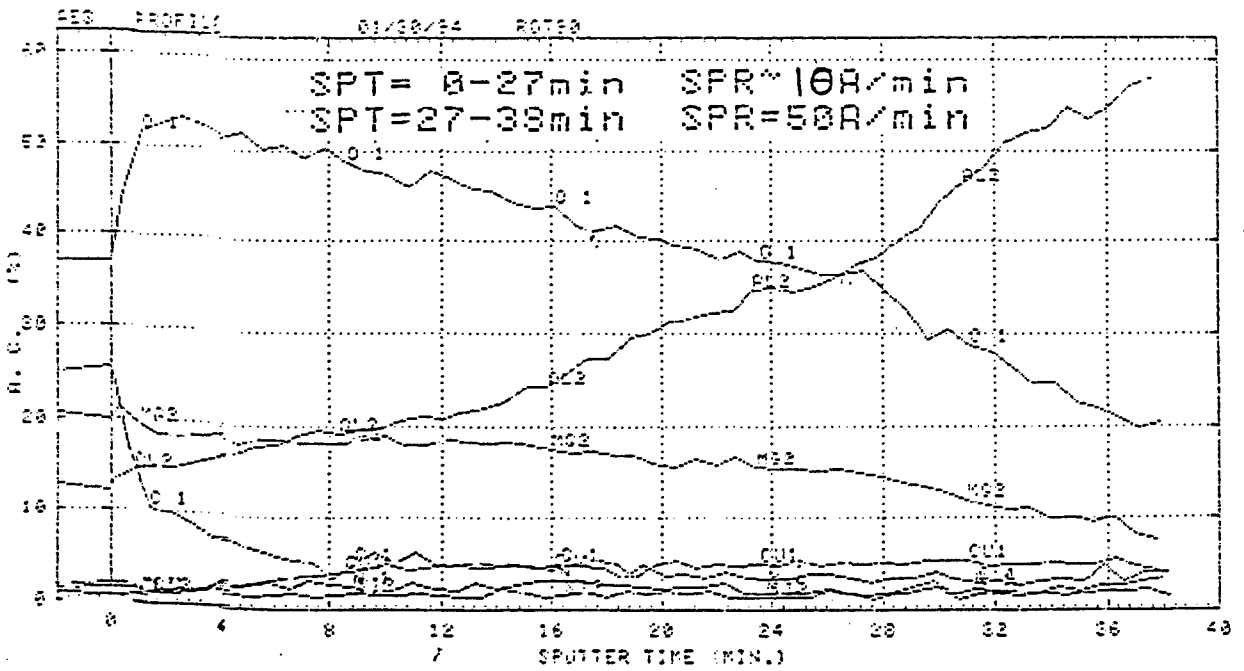
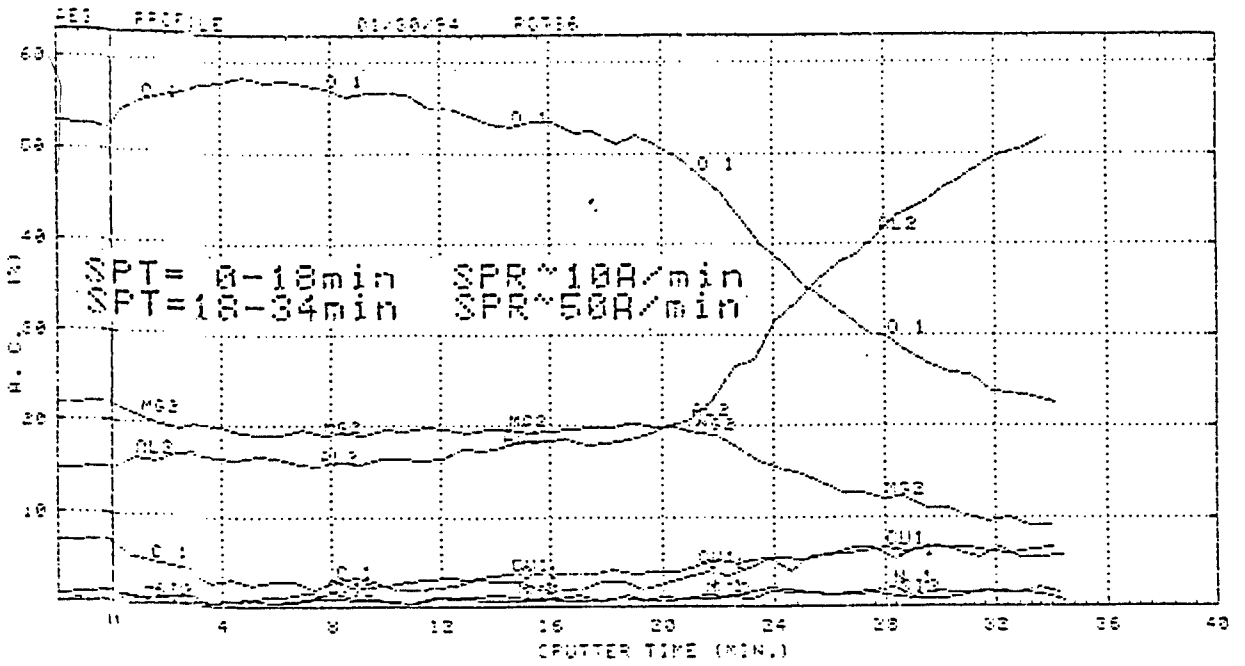


Fig. 3.19: Auger depth profile of Al irradiated at laser energy of $0.18\text{J/p}\cdot\text{cm}^2$. a. 2000 pulses b. 5000 pulses.

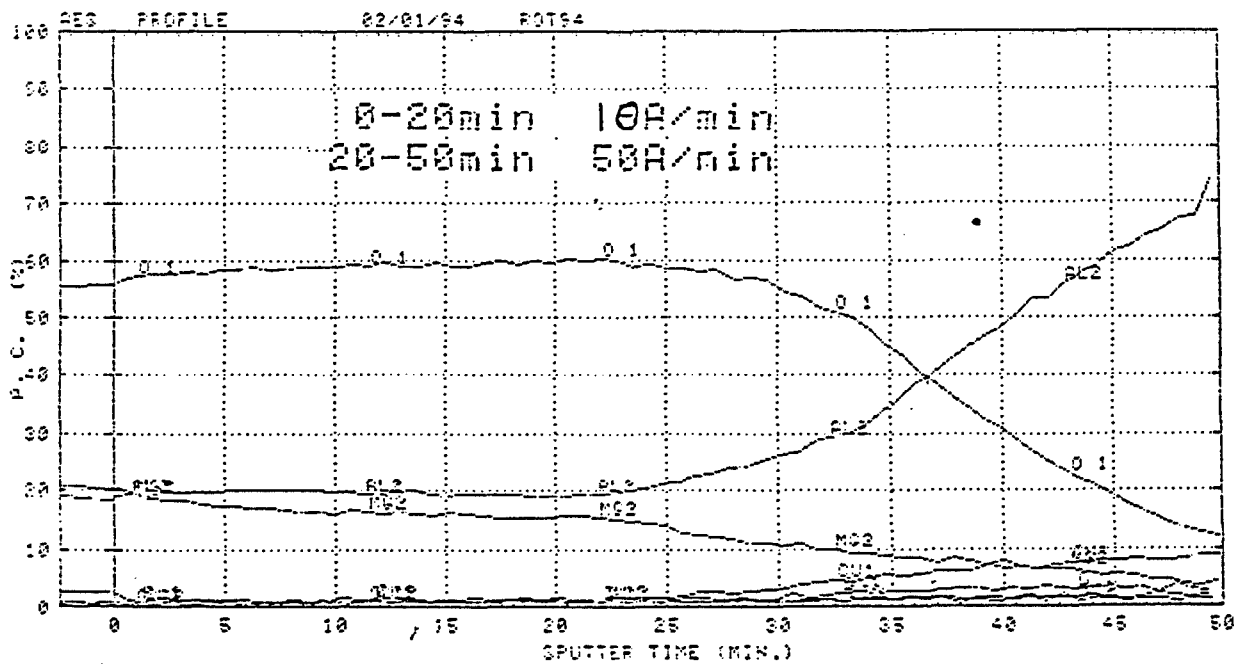
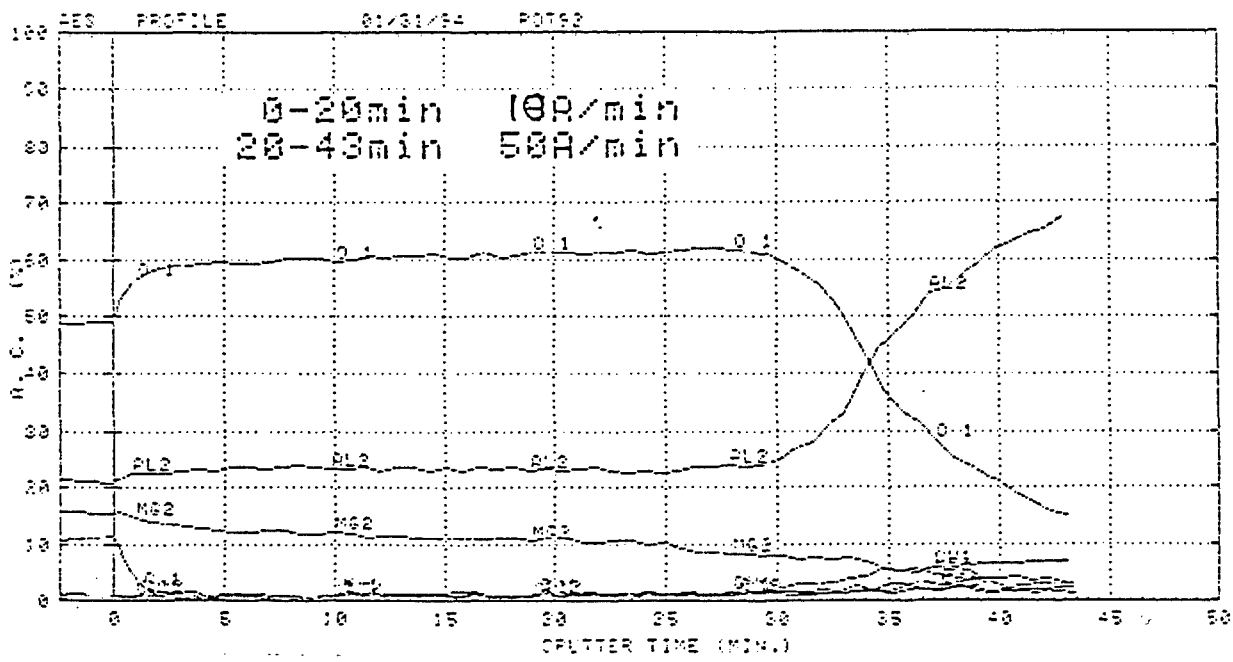


Fig. 3.20: Auger depth profile of Al irradiated at laser energy of 0.57J/p*cm². a.10 pulses b.1000 pulses.

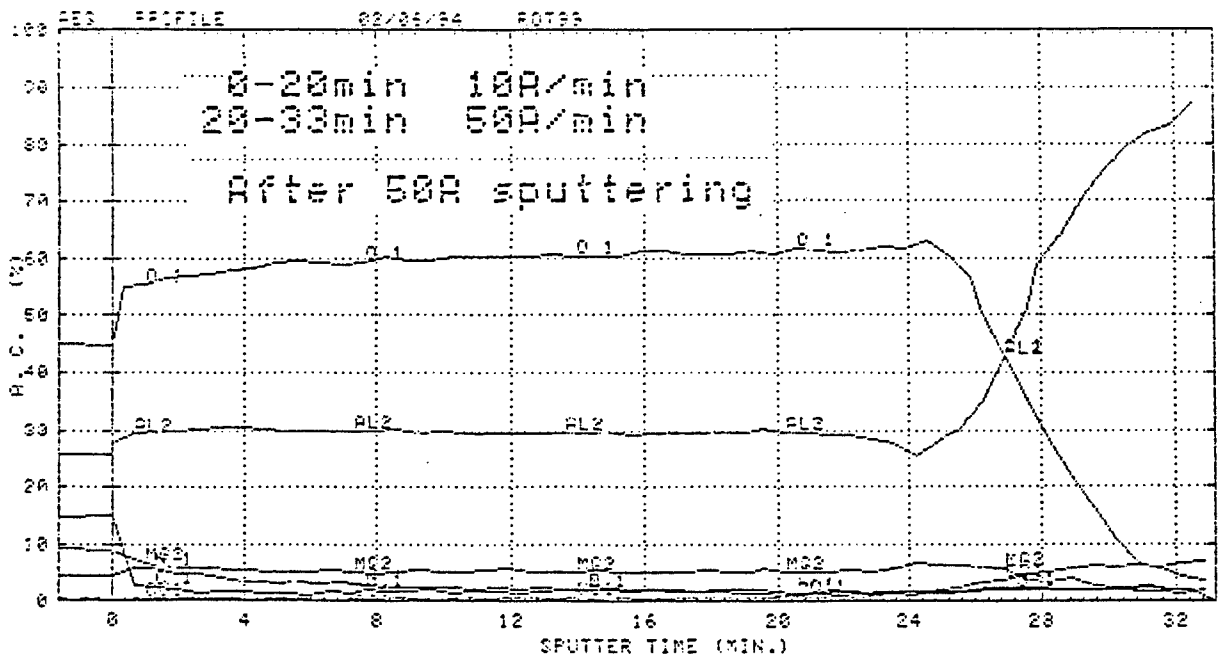
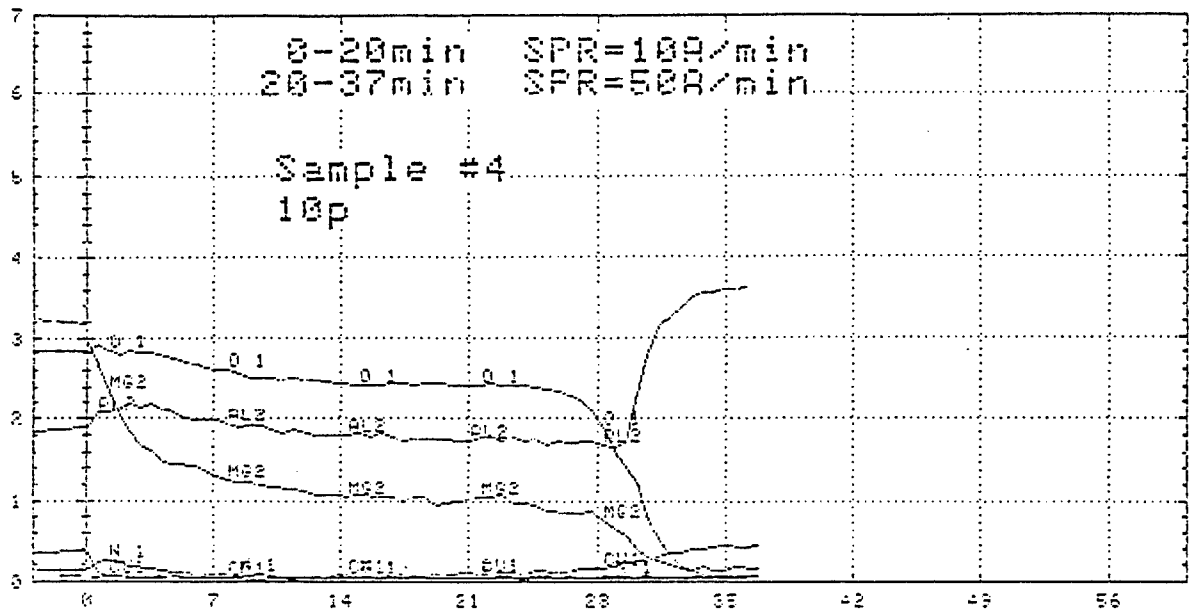


Fig. 3.21: Auger depth profile of Al irradiated at laser energy of $1\text{J/p}\cdot\text{cm}^2$. a. 10 pulses b. 100 pulses.

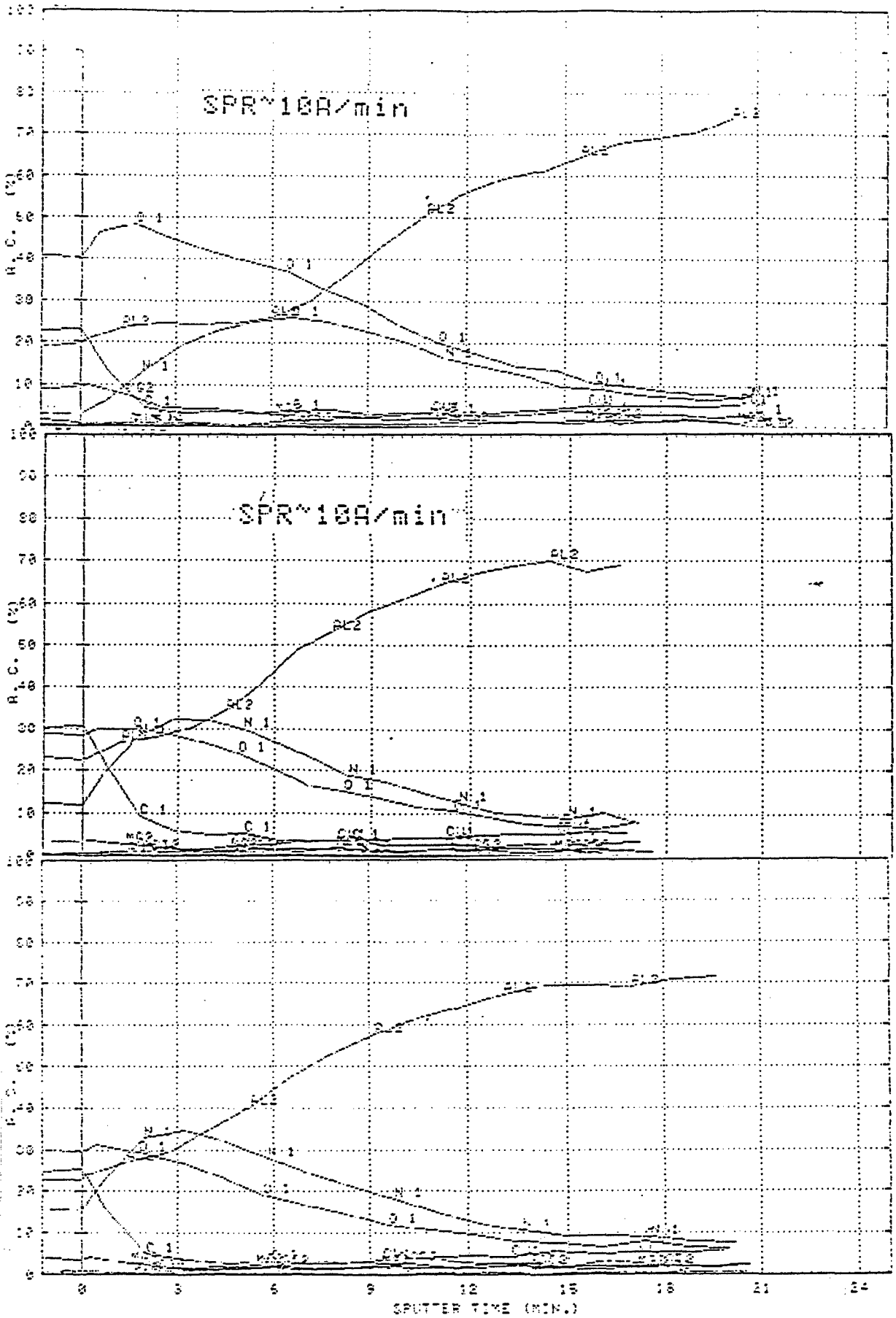


Fig. 3.22: Auger depth profile of Al irradiated at laser energy of 2.7J/p*cm². a. 10 pulses b. 50 pulses. c. 100 pulses.

3.4 Contact Angle Measurement

In any kind of adhesion, wetting the surface by the adhesive is important. The common way to characterize the surface activity is by measurement of contact angle. A drop of liquid is placed on the adherend and contact angle is measured at the point where the two phases meet (solid/liquid). Perfect wetting occurs when $\cos\theta=1$ ($\theta=0$). The lower is θ the better is the wetting. Contact angles of treated and untreated Al adherends were measured with water drops on a Contact Angle instrument .

Laser treatment caused significant decrease in the contact angle compare to untreated Al, which shows improved wetting after laser treatment. Table 3.6 summarized these results. Contact angle with various other liquids will be measured in order to evaluate changes in critical surface tension (γ_c) due to laser treatment.

Table 3.6: Effect of laser treatment on contact angle between water and laser treated aluminum.

Sample	Laser energy J/p·cm ²	Pulses No.	Contact angle, θ°
Untreated	-	-	90
Laser treated	0.18	100	58
		600	52
		1000	43
		2000	41.6
		5000	43
	1	1	56
		10	59
		100	52
	4	1	51
		10	62

4. SUMMARY

The third stage of this research (0003 of the contract) is summarized in the report. This stage included characterization of failure modes following shear tests compared to the strength results of the shear tests which were reported in the previous report (second stage report). Chemical changes on substrate surface are evaluated and reported. It can be concluded that:

- Adhesion strength with laser treated adherends improved by more than 150% compared to untreated Al, and was close to the shear strength of the anodized Al.
- Cohesive surfaces were observed with SEM after laser treatment.
- FTIR and auger spectroscopy showed oxides formation and their nature and cleaning of the surface from contaminations.
- Contact angle between water and Al decrease as a result of laser treatment.
- The preferred laser treatment for Al2024 adherend is: $0.18\text{J/p}\cdot\text{cm}^2$ with 2000 pulses at repetition rate of 30Hz.

REFERENCES

1. M. Rotel, J. Zahavi, H. Dodiuk, A. Buchman, "Laser induced reaction for pre-bond surface treatments of aluminium alloys", Annual Report, March 1992.
2. H. Dodiuk, A.E. Yaniv and N. Fin, "Characterization of oxidized Al-1100 exposed to hygrothermic environments", Applied Surface Science 29, 1987, pp. 67-85.
3. N. Fin, H. Dodiuk, A.E. Yaniv and L. Drori, "Oxide Treatments of Al 2024 for adhesive bonding - surface characterization", Applied Surface Science 28 (1987), pp. 11-13.
4. W.K. Wafers, C. Misra, "Oxides and Hydroxides of Aluminum", Acoa Laboratories, 1987.
5. Kh.N. Numagambctov et al., "Infrared spectroscopy study of phase transformations in the aluminum-hydroxide system", Metallurgiya Obogashchenie, 1974, pp. 18-22.
6. Int. J. Adhesive, Adhesives 10,(4), 254, (1990).